

# CONCEPTUAL DESIGN OF AN ELECTROSTATIC TRAP FOR HIGH INTENSITY PULSED BEAM\*

W. Huang†, L. T. Sun, Y. G. Liu and H. W. Zhao

University of Chinese Academy of Sciences/IMP/CAS, Lanzhou, China

D. Z. Xie, LBNL, USA

## Abstract

Highly charged ion sources play an important role in the advancement of heavy-ion accelerators worldwide. Demands of highly-charged heavy ions for new and existing accelerators have driven the performance of ion sources to their limits and beyond. In parallel to developing new technologies to enhance the performance of ECR ion source, this paper presents a conceptual design of an ion trap aiming to convert a CW ion beam into a short beam pulse with high compression ratios. With an electron gun, a solenoid and a set of drift tubes, the injected ions will be trapped radially and axially. By manipulating the potential of the drift tubes, ions can be accumulated with multiple injections and extracted at a fast or a slow manner. This paper presents the simulations and design features of the envisioned ion trap.

## INTRODUCTION

The ion kinetic energy produced with accelerators is either proportional to the square of the ion charge state  $Q$  (Cyclotrons) or linear to  $Q$  (Linac). Therefore, if the beam intensity can meet the requirement, future and existing heavy-ion accelerators can benefit from injecting ion beams of higher charge state  $Q$  which could not only achieve the required accelerator performance but also possibly lead to substantial cost savings. After more than 40 years' continued development, the state of the art Electron Cyclotron Resonance Ion Source (ECRIS) has advanced to a 3<sup>rd</sup> generation with full-superconducting magnets operating at 24 to 28 GHz microwaves, such as VENUS at LBNL, SECRAL & SECRAL 2 at IMP, SC-ECR at RIKEN and SUSI at MSU, etc. [1-5] To advance science research and enhance its capabilities, future and existing heavy-ion accelerators worldwide demand intense highly-charged ion beams. For example, FRIB at MSU needs 13  $\mu\text{A}$  of CW (continuous wave)  $^{238}\text{U}^{34+}/\text{U}^{33+}$  [6], FAIR at GSI needs 15 emA of pulsed  $^{238}\text{U}^{28+}$  beam [7], High Intensity heavy ion Accelerator Facility (HIAF) at IMP needs  $\text{U}^{34+}$  ion beams with an intensity of 1.7 emA in pulsed mode [8], which is far beyond the record what SECRAL 2 can achieve, 390  $\mu\text{A}$  of  $\text{U}^{34+}$  [9].

Presently the 4<sup>th</sup> generation of ECR ion source is under development to meet the heavy ion beam intensity demands with as high charge state as possible. The development of the next generation of ECR ion source requires great efforts/resources and is a time consuming process as it has to overcome many technical challenges, such as how

to fabricate the magnet system to mitigate the much higher em interaction forces, more demanding quench protection, sufficient cooling the plasma chamber under high microwave power operation, etc. [10] While benefitting from the 4<sup>th</sup> generation ECR ion sources, those heavy-ion accelerators requiring intense pulsed ion beams can also benefit from a relatively low-cost device that can convert a CW ion beam of lower intensity but with higher charge state into an intense beam pulse. This is the reason we plan to develop a CW ion beam compressor that could trap and accumulate the highly-charged ions from an ECR ion source to convert those ions into a much higher peak intensity pulsed beam. The simulation details of this conceptual Ion TRap for high Intensity Pulsed beams (ITRIP) are presented and discussed below.

## PRINCIPLE OF THE ION TRAP

The structure of the ion trap is very similar to an Electron Beam Ion Source (EBIS), as schematically shown in Fig. 1. Highly charged ions produced with an ECR ion source are injected into the ion trap where the ions get slowed down for accumulation and extraction. A cathode of high emissivity produces an electron beam to provide a negative potential well to radially confine the ions. The axial confinement of the ions is achieved by 1. a high gate potential at the left end (as shown in Fig. 1) to keep the ions from escaping the Trapping Section; 2. a set of drift tubes at the injection side (Bunching Section) to generate a repeating traveling electric potential wave ( $V_{\text{bunch}}(f)$ ) to accept and move the ions into the Trapping Section and at the same time minimize the ion axial escaping. The Trapping Section accumulates the ions until the ions are extracted out, through manipulating the electric potential at the left hand and other electrodes, to form an intense beam pulse.

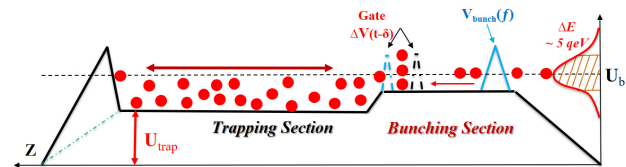


Figure 1. Schematic layout of the ion trap.

The most important key factor of the ion trap is the ion trapping efficiency. Some of the ions will get lost during the accumulation and extraction periods. The ion trap should preserve the ion charge state, in addition to confining the ions. The charge state of ions can be lower due to charge exchange with the background gas, radiative recombination (RR) with the electrons, etc. An ultrahigh vacuum should be provided to reduce the charge exchange. Some of the electrons will also get trapped moving back

\* Work supported by the program of China Scholarships Council (No. 201904910324).

† whuang@impcas.ac.cn

and forth which leads to an increased electron density resulting in higher space charge potential for better ion confinement.

The repetition rate requirement for HIAF is 1 Hz with an injection time of about 400  $\mu$ s and the CW beam intensity of  $U^{34+}$  or higher charge state uranium ions is typically 0.2 to 10's  $\mu$ A produced with SECRAL 2 ion source. So if the ion trap can catch 50% of an injected 1  $\mu$ A of  $U^{34+}$  ions in the Bunching Section and with a 25% accumulation efficiency in the Trapping Section, the number of  $U^{34+}$  ions in the Trapping Section would be  $\sim 7 \times 10^{11}$  assuming the capacity of Trapping Section is high enough. If the extraction efficiency of the ion trap can reach 50% which would lead to  $\sim 3.5 \times 10^{11}$  ions/pulse.

## DESIGN OF THE ELECTRON GUN

A magnetic field is needed for confinement of the electrons. To minimize the simulation time for the conceptual design, the length of the ITRIP is chosen to be  $\sim 0.5$  m. The magnetic field is produced by a solenoid located inside an iron yoke, as shown in Fig. 2 (a). The current density of solenoid is 9 A/mm<sup>2</sup>. The inner and outer radius of solenoid are 10 cm and 15 cm, respectively. The length of solenoid is 0.5 m. The thickness of the iron yoke is 2 cm. The computed magnetic field distribution with Vector Field TOSCA [11] is shown in Fig. 2 (b). The maximal magnetic field in the trap is  $\sim 5570$  G which can be produced by room temperature solenoid with water cooling.

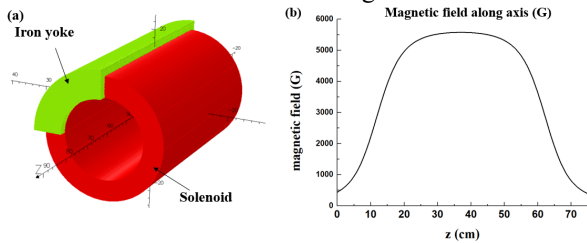


Figure 2. (a) Magnet structure. (b) Magnetic field profile.

Ions are to be injected from one side and extracted from the other side of the ion trap. An electron hollow cathode of a convex surface located at the extraction end is designed with an adequate aperture for ion extraction. A portion of the electron beam, with energy loss due to collision, is trapped between the cathode and reflecting electrode in the confining magnetic field. The corresponding thermionic current density on the cathode is described by Richardson-Dushman as follows [12]:

$$j = A_G T^2 \exp\left(-\frac{\phi}{k_B T}\right) \quad (1)$$

Where  $A_G$  is generalized Richardson constant,  $T$  is the cathode temperature in K,  $\phi$  is the work function in eV and  $k_B$  is Boltzmann constant.

The radius of drift tube along axis should meet the following equation to maintain a uniform potential distribution in the trap with the same potential on all drift tubes [13]:

$$R_i(z) = R_{i,0} \cdot \sqrt{\frac{B_0}{B(z)}} \quad (2)$$

Where  $R_i(z)$  is the inner radius of drift tubes at a location of axial coordinate  $z$  and magnetic field  $B(z)$  and  $R_{i,0}$  is in the point with the maximum value of  $B(z)$ , notated as  $B_0$ .

LaB<sub>6</sub> is widely used in fabricating thermionic electron cathode. Its operating temperature is over 1500 K with generalized Richardson constant of 29 A $\cdot$ cm<sup>-2</sup> $\cdot$ K<sup>-2</sup> [14]. The anode consists of two rings to let electron go through between them. The electron gun is simulated with Vector Field SCALA [11]. The hollow electron beam oscillates between the cathode and reflecting electrode, i.e., back and forth through the Trapping Section and the Bunching Section. To get a convergent result, the 9<sup>th</sup> drift tube and the reflecting electrode after that are omitted in the simulation, as shown in Fig. 3. The temperature of cathode in simulation is 1600 K, the relative potential of all the electrodes including cathode from left to right are 0, 2.5 kV, 4 kV, 1.1 kV, 1.1 kV, 1.1 kV, 1.1 kV, 2.5 kV, 1.1 kV, 1.1 kV. The potential of gate electrode is 2.5 kV when it's closed.

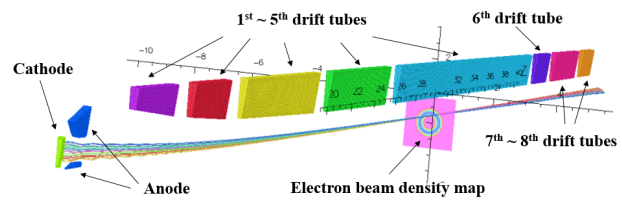


Figure 3. Simulation result of the electron gun.

The electron beam current is  $\sim 430$  mA according to the simulation, with inner  $r_1$  of  $\sim 0.3$  cm and outer radius  $r_2$  of  $\sim 0.46$  cm, as shown in Fig. 4 (a). The trap potential of an electron beam with uniform distribution of radius  $r_e$  has the shape [15]

$$V_e(r) = \begin{cases} \frac{U_e r^2}{r_e^2} & \text{for } r \leq r_e \\ U_e \left(2 \ln \frac{r}{r_e} + 1\right) & \text{for } r > r_e \end{cases} \quad (3)$$

Where  $U_e = I_e / (4\pi\epsilon_0 v_e)$ . The hollow electron beam shown in Fig. 4 (a) can be regarded as a combination of a positive electron beam with radius of  $r_1$  and a negative electron beam with radius of  $r_2$ . Assume the relative potential on the drift tube with radius  $R_i$  is 0, the space charge potential of the hollow electron beam of 430 mA and 1.1 keV can be calculated with equation (3), as shown in Fig. 4 (b). The depth of the space charge potential of electrons is  $\sim 0.29$  kV. Increase the beam current can increase the potential depth which can lead to better ion confinement.

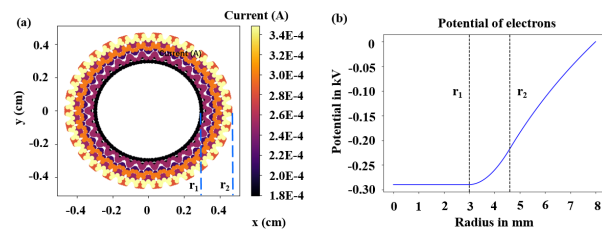


Figure 4. Space charge potential distribution according to the current distribution of electrons. (a) Current distribution. (b) Space charge potential of electron beam.

## SIMULATION OF THE ION TRAP

Assume the energy of  $U^{34+}$  ions at the exit of an ECRIS are the same which is  $21.13 \cdot q$  keV where  $q$  is the charge state. The energy of  $U^{34+}$  ions will be decreased to  $0.03 \cdot q$  keV if the 8<sup>th</sup> drift tube is on 21.1 kV. Assume a parallel beam of  $U^{34+}$  of radius of 5 mm prior to its injection into the ion trap with magnetic field, Fig. 5 shows the simulation of the injected  $U^{34+}$  beam profile with code IBSIMU [16]. The electron beam in the trap is omitted to simplify the simulation. The potential of these 4 electrodes from left to right are 17 kV, 20.7 kV, 21.1 kV, 21.1 kV. The potential of the left boundary is 0 V. The left boundary, reflecting electrode and the 9<sup>th</sup> drift tube can be regarded as an einzel lens that focus ion beam at injection.

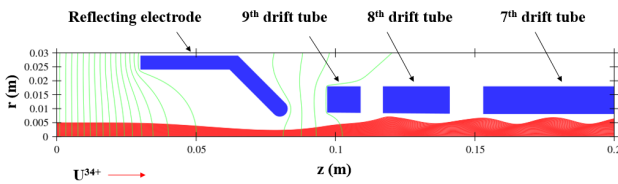


Figure 5. Simulated profile of  $U^{34+}$  ions injection.

A PIC simulation software VSim [17] is used to simulate the accumulation of ions in the trap with electrons and the process is extremely time consuming. To get a feel of the trapping, the collisions including charge exchanges and RR (Radiative Recombination) processes among the particles are neglected but take into account the effects of the em field and space charge force on the  $U^{34+}$  ions. The electrostatic potential varies depending on the space charge potential of electron beam. The energy of  $U^{34+}$  ions can vary from  $(10 \sim 100) \cdot q$  eV in the Bunching Section.

Potential on the 9<sup>th</sup> drift tube will be raised to trap the ions when the Bunching Section is full. Potential on the 8<sup>th</sup> drift tube will be raised when compressing the ions. Potential on the 6<sup>th</sup> drift tube will be lower (the gate is open) to dump the  $U^{34+}$  ions into the Trapping Section when compression of ions is completed. Potential on the 7<sup>th</sup> potential will be raised to push the remaining ions into the Trapping Section, and potential on the 6<sup>th</sup> potential will be raised (the gate is closed) after that. Repeat these processes several times until the Trapping Section is full. The trajectory of one bunch of  $U^{34+}$  at  $9.6 \mu s$  when dumping of ions is completed is shown in Fig. 6 (a). The green points are electrons and the red points are  $U^{34+}$  ions in which a good portion of the ions is trapped. The velocity distribution of ions along axis is shown in Fig. 6 (b). Some of the ions with larger energy are reflected by the 1<sup>st</sup> drift tube while the lower energy ions remain in the Bunching Section.

Due to the time consuming computation and the capability limit of a desktop computer, only 5 bunches of  $U^{34+}$  ions are conducted in the simulations. The time for each bunch in injection is  $\sim 10 \mu s$  which consists of  $\sim 3 \mu s$  of injection time,  $\sim 4 \mu s$  of compression time and  $\sim 3 \mu s$  of dumping time. The accumulation results of electrons and  $U^{34+}$  ions in the trap are shown in Fig. 7. The accumulation of electrons is essentially saturated after  $40 \mu s$  with electrons of  $\sim 5 \times 10^{12}$  in the trap, which means the theoretical capacity of

the trap for  $U^{34+}$  is  $\sim 1.4 \times 10^{11}$  that should be increased further. The calculated number of trapped  $U^{34+}$  ion at  $50 \mu s$  is  $\sim 1.8 \times 10^8$  in the simulation. A fitting plot of quadratic function predicts the number of trapped  $U^{34+}$  ions to reach  $3.4 \times 10^{10}$  after 1 s, which is only a quarter of the theoretical capacity of the trap. Assume the extraction efficiency is  $\sim 50\%$ , the intensity of  $U^{34+}$  after extraction without considering charge exchange and RR processes will be  $1.7 \times 10^{10}$  ions/pulse.

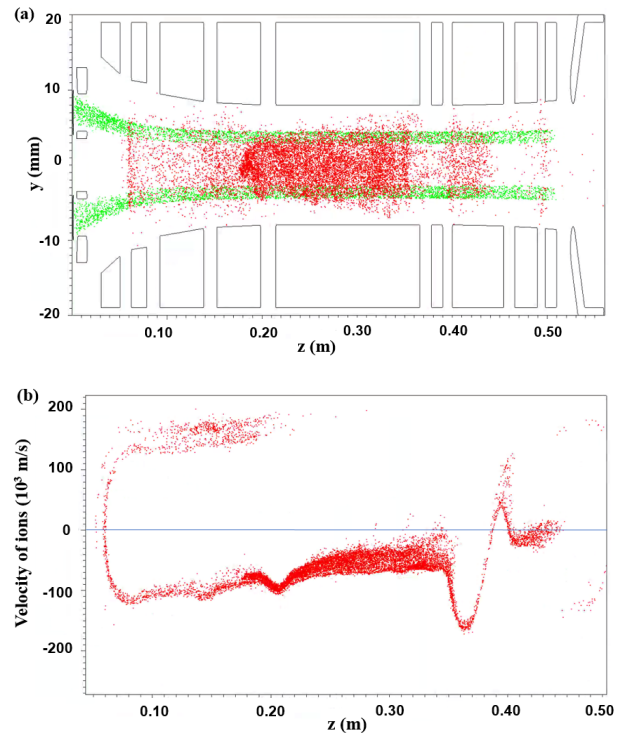


Figure 6. Simulation of one bunch of injection. (a) Particle distributions. (b) Ion velocity distribution.

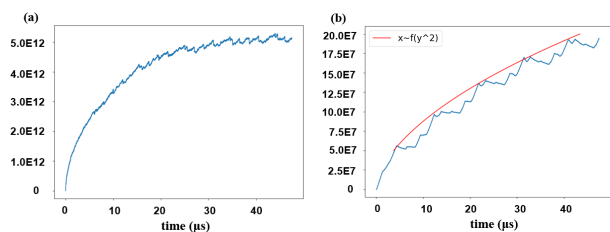


Figure 7. Simulation of the accumulation of electrons (a) and  $U^{34+}$  ions (b).

The ions will be extracted from the ion trap at 1 s to accommodate HIAF injection frequency. To simulate the extraction of a high intensity ion beam, assume the extracted instantaneous peak current of  $U^{34+}$  is 1 A with  $150 \cdot q$  eV, the simulated result is shown in Fig. 8. The outer ring of anode is omitted for simplicity. An einzel lens is used to focus the  $U^{34+}$  ions to mitigate the strong space charge force. During the extraction, the voltage of anode decreases to 21.1 kV while the voltage of cathode remains on 20 kV. The voltages of einzel lens from left to right are 19.1 kV, 11.1 kV, 10.1 kV.

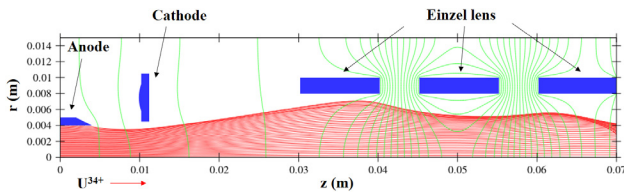


Figure 8. Simulated profile of  $U^{34+}$  ions extraction.

## DISCUSSION

The capacity of the discussed trap for both electrons and ions is proportional to the trap length to certain extent that means a higher trapping capacity feasible with a longer trap. A larger line density of electrons will lead to a better confinement for ions, which means the current of electron gun can be higher. Increasing the voltage of the anode is a direct way to get a higher current electron beam. However, a too high electron energy can lead to ion ionization resulted in ion loss.

The balance equation of ions considering ionization, RR, charge exchange and the loss of heated ions by Coulomb collisions can be found in reference [18]. Consider the evolution of charge state of uranium ions in 3 cases: (a) 0.15A of electrons with 500 eV in the trap; (b) 0.5 A of electrons with 1100 eV in the trap; (c) 4.7 A of electrons with 5000 eV in the trap. Assume the initial  $U^{34+}$  ions in the trap is  $3.4 \times 10^{10}$ , namely  $\sim 6 \times 10^8 \text{ cm}^{-3}$  in the trap for a confining column of cross section of  $\sim 1 \text{ cm}^2$ . At a background vacuum of  $1 \times 10^{-10}$  Torr, the calculated charge state evolution of uranium ions for the 3 cases mentioned above are shown in Fig. 9. In the 1<sup>st</sup> case (Fig. 9 (a), (d)), the loss of  $U^{34+}$  ions due to charge exchange and RR processes makes up only 3% of the total loss, which means  $U^{34+}$  ions are lost mainly due to poor confinement caused by the low current of electrons. In the 3<sup>rd</sup> case (Fig. 9 (c), (f)), The loss of  $U^{34+}$  ions due to charge exchange and RR processes makes up almost the total loss, which means the confinement for ions is good enough. Some  $U^{34+}$  ions are ionized, as the ionization potential of  $U^{34+}$  is only 1.4 keV, by the high energy of electrons resulted in more loss of  $U^{34+}$  in comparison to the 2<sup>nd</sup> case (Fig. 9 (b), (e)) after 10 ms. The loss of  $U^{34+}$  ions due to charge exchange and RR processes makes up 40% of the total loss in case 2 and goes up as increase the current of electron beam. Increasing the energy of electrons to get a higher electron beam current is feasible but the electron energy should depend on the tolerable loss of ions to be trapped.

Assume the  $U^{34+}$  ions accumulate as the fitting curve in Fig. 7 (b), the evolution of charge state of ions considering only charge exchange and RR processes is shown in Fig. 10 with an electron beam current of 0.4 A and 1100 eV when the vacuum is  $1 \times 10^{-10}$  Torr. The trapped U ions will be  $1.24 \times 10^{10}$  after 1 s. As a result, the intensity of  $U^{34+}$  for ITRIP after extraction will be  $6.2 \times 10^9$  ions/pulse with an extraction efficiency of 50% and that means more efforts needed to increase output.

Experimental proof of principle is needed to verify the validity of the design. The structure design of the ITRIP is

almost completed, the machining and experiments will be taken place in the near future.

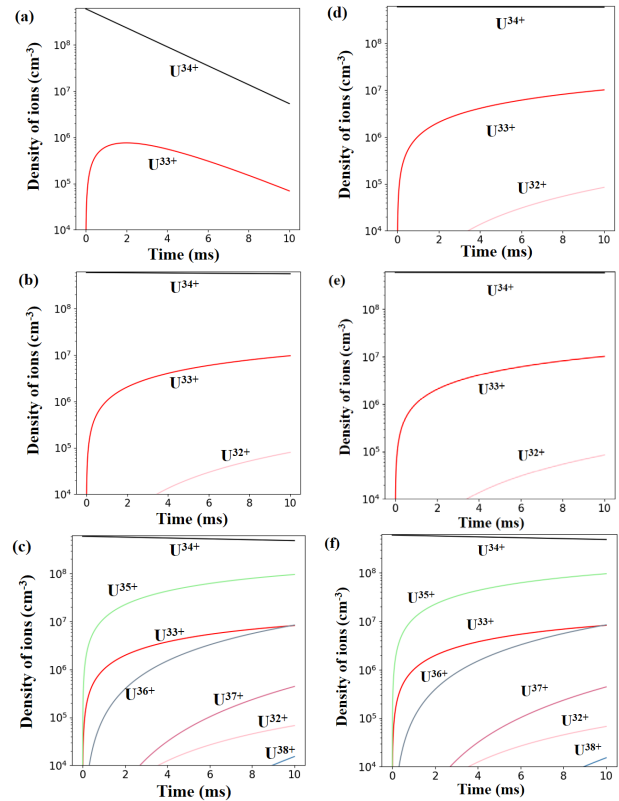


Figure 9. Evolution of charge state of ions for different cases considering all the loss processes (a), (b), (c) and only charge exchange, RR processes (d), (e), (f).

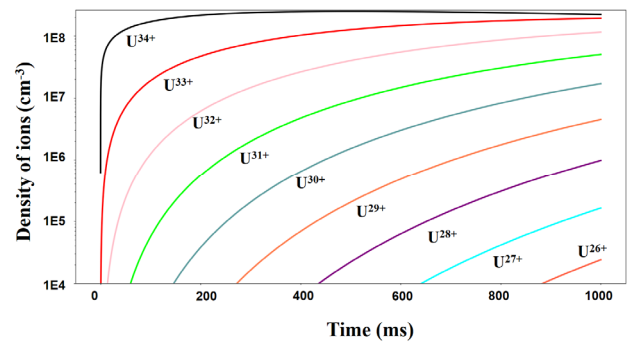


Figure 10. Evolution of charge state of ions in 1 s.

## ACKNOWLEDGEMENTS

This work has been supported by the program of China Scholarships Council (No. 201904910324).

## REFERENCES

- [1] J. Y. Benitez et al., "Current Developments of the VENUS Ion Source in Research and Operations", in Proc. 20th Int. Workshop on ECR Ion Sources (ECRIS'12), Sydney, Australia, Sep. 2012, paper THX002, pp. 153-158.
- [2] H. W. Zhao et al., "New development of advanced superconducting electron cyclotron resonance ion source

- SECRAL”, *Rev. Sci. Instrum.* Vol. 81, p 02A202, 2010.  
doi: 10.1063/1.3273058
- [3] L. T. Sun et al., “SECRAL II Ion Source Development and the First Commissioning at 28 GHz”, in *Proc. 22nd Int. Workshop on ECR Ion Sources (ECRIS'16)*, Busan, Korea, Aug.-Sep. 2016, pp. 43-47.  
doi:10.18429/JACoW-ECRIS2016-TUA004
- [4] Y. Higurashi et al., “Recent development of RIKEN 28 GHz superconducting electron cyclotron resonance ion source”, *Rev. Sci. Instrum.* Vol. 85, p 02A953, 2014.  
doi: 10.1063/1.4848976
- [5] G. Machicoane et al., “Performance Investigation of the NSCL 18 GHz Superconducting ECR Ion Source SUSP”, in *Proc. 23rd Particle Accelerator Conf. (PAC'09)*, Vancouver, Canada, May 2009, paper MO6RFP035, pp. 432-434.
- [6] J. Wei, “The Very High Intensity Future”, in *Proc. 5th Int. Particle Accelerator Conf. (IPAC'14)*, Dresden, Germany, Jun. 2014, pp. 17-22.  
doi:10.18429/JACoW-IPAC2014-MOYBA01
- [7] O. K. Kester, “Status of the FAIR Facility”, in *Proc. 4th Int. Particle Accelerator Conf. (IPAC'13)*, Shanghai, China, May 2013, paper TUXB101, pp. 1085-1089.
- [8] X. Guoqing et al., “HIAF and CiADS National Research Facilities: Progress and Prospect”, *Nucl. Phys. Rev.*, Vol. 34, p. 275283, 2017.  
Doi: 10.11804/NuclPhysRev.34.03.275
- [9] W. Lu et al., “Production of intense uranium beams with inductive heating oven at Institute of Modern Physics”, *Rev. Sci. Instrum.*, vol. 90, p. 113318, 2019.  
doi: 10.1063/1.5128419
- [10] H. W. Zhao et al., “Superconducting ECR ion source: From 24-28 GHz SECRAL to 45 GHz fourth generation ECR”, *Rev. Sci. Instrum.*, vol. 89, p. 052301, 2018.  
doi: 10.1063/1.5017479
- [11] OPERA 3d, Vector Fields Ltd., <https://www.3ds.com/products-services/simulia/products/opera/>.
- [12] A. Modinos, *Field, Thermionic and Secondary Electron Emission Spectroscopy*, New York, USA: Springer, 1984.
- [13] A. I. Pikin et al., “Tandem EBIS”, in *Proc. 12th Int. Conf. on Heavy Ion Accelerator Technology (HIAT'12)*, Chicago, IL, USA, Jun. 2012, paper PO18, pp. 101-104.
- [14] K. Torgasin et al., “Thermally assisted photoemission effect on CeB<sub>6</sub> and LaB<sub>6</sub> for application as photocathodes”, *Phys. Rev. Accel. Beams*, vol. 20, p. 073401, 2017.  
doi: 10.1103/PhysRevAccelBeams.20.073401
- [15] G. Zschornacka et al., “Electron Beam Ion Sources”, *CERN Accelerator School (CAS)*, Senec, Slovakia, May – Jun. 2012.  
doi: 10.5170/CERN-2013-007.165
- [16] T. Kalvas et al., “IBSIMU: A three-dimensional simulation software for charged particle optics”, *Rev. Sci. Instrum.*, vol. 81, p. 02B703, 2010  
doi: 10.1063/1.3258608.
- [17] VSim, Tech-X, <https://www.txcorp.com/vsim/>.
- [18] R. Becker et al., “Simulation of charge breeding for trapped ions”, *J. Phys.: Conf. Ser.*, vol. 58, p. 443, 2007.  
doi: 10.1088/1742-6596/58/1/102